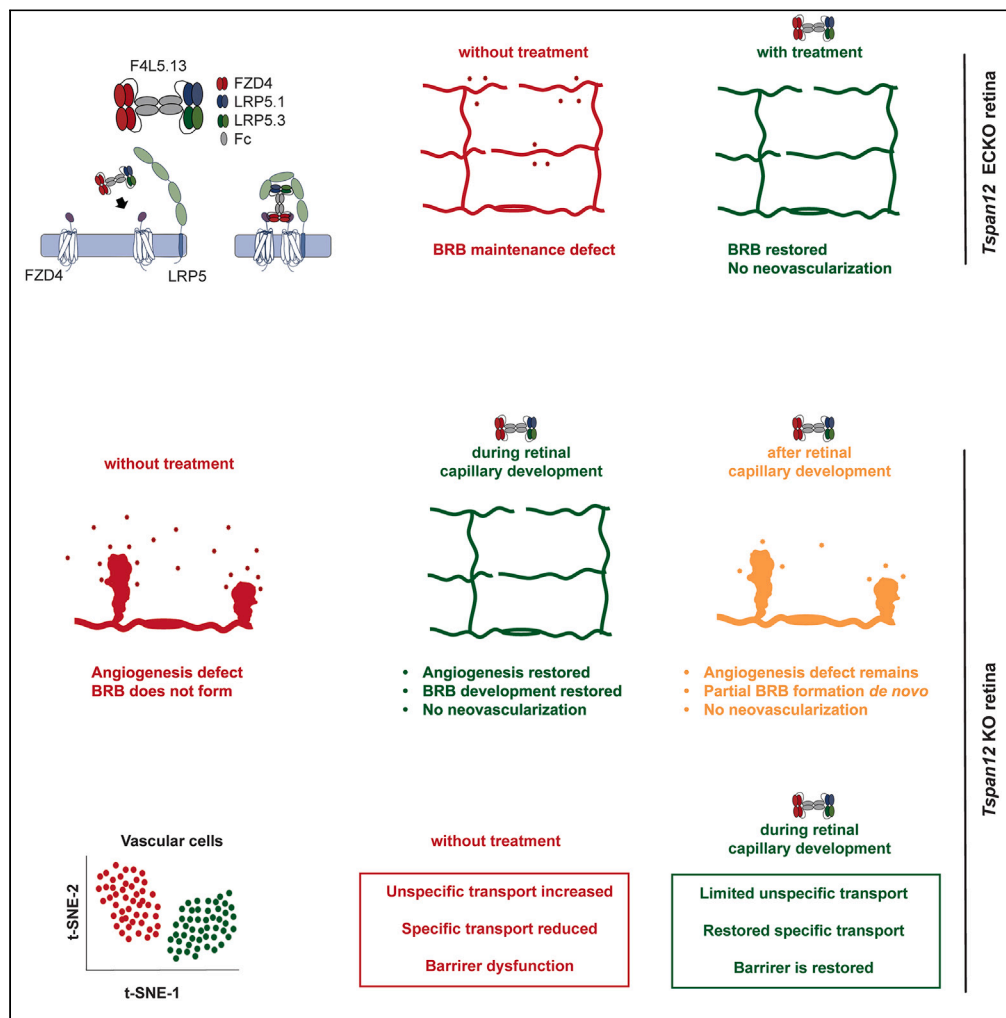


Article

# A Frizzled4-LRP5 agonist promotes blood-retina barrier function by inducing a Norrin-like transcriptional response



Lingling Zhang, Md. Abedin, Ha-Neul Jo, ..., Zhe Chen, Stephane Angers, Harald J. Junge

zhangll@umn.edu (L.Z.)  
 junge@umn.edu (H.J.J.)

Highlights

Frizzled4-LRP5 agonist mimics Norrin in retinal angiogenesis and barriergenesis

Induces *de novo* barrier formation in adult mice after failed barrier development

Proangiogenic effects are context-dependent and are limited to development

Transcriptional regulation of endothelial cell differentiation and transport



## Article

## A Frizzled4-LRP5 agonist promotes blood-retina barrier function by inducing a Norrin-like transcriptional response

Lingling Zhang,<sup>1,\*</sup> Md. Abedin,<sup>1</sup> Ha-Neul Jo,<sup>1,2</sup> Jacklyn Levey,<sup>1,2</sup> Quynh Chau Dinh,<sup>1</sup> Zhe Chen,<sup>3</sup> Stephane Angers,<sup>4,5,6</sup> and Harald J. Junge<sup>1,2,7,\*</sup>

## SUMMARY

**Norrin (NDP) and WNT7A/B induce and maintain the blood-brain and blood-retina barrier (BBB, BRB) by stimulating the Frizzled4-LDL receptor related protein 5/6 (FZD4-LRP5/6) complex to induce beta-catenin-dependent signaling in endothelial cells (ECs). Recently developed agonists for the FZD4-LRP5 complex have therapeutic potential in retinal and neurological diseases. Here, we use the tetravalent antibody modality F4L5.13 to identify agonist activities in *Tspan12*<sup>-/-</sup> mice, which display a complex retinal pathology due to impaired NDP-signaling. F4L5.13 administration during development alleviates BRB defects, retinal hypovascularization, and restores neural function. In mature *Tspan12*<sup>-/-</sup> mice F4L5.13 partially induces a BRB *de novo* without inducing angiogenesis. In a genetic model of impaired BRB maintenance, administration of F4L5.13 rapidly and substantially restores the BRB. scRNA-seq reveals perturbations of key mediators of barrier functions in juvenile *Tspan12*<sup>-/-</sup> mice, which are in large parts restored after F4L5.13 administration. This study identifies transcriptional and functional activities of FZD4-LRP5 agonists.**

## INTRODUCTION

The BBB and BRB regulate transport at the interface of the circulatory system and the CNS. These barriers limit the nonspecific movement of solutes and instead provide specific transport mechanisms for nutrients, hormones, and waste products. BBB and BRB protect the CNS from harmful plasma components and contribute to the CNS immune privilege. Several major retinal diseases are associated with BRB dysfunction, including diabetic macular edema, neovascular age-related macular degeneration, and retinal vein occlusion, as well as rare congenital diseases such as familial exudative vitreoretinopathy (FEVR) and Norrie disease.<sup>1–3</sup> Among the neurological diseases associated with BBB dysfunction are stroke, traumatic brain injury, neurodegenerative diseases, CNS tumors, and epilepsy.<sup>4–9</sup> Barrier dysfunction may have a predominant role in driving pathological states (e.g., in macular edema), or constitute an exacerbating factor that worsens the outcome. Therapeutic interventions that target permeability-inducing factors in retinopathies, e.g., VEGF,<sup>10</sup> have been developed. However, an intervention that actively promotes or restores barrier function is lacking. Drug candidates that promote BRB functions have the potential to address an unmet medical need in case anti-VEGF is not effective or patients develop resistance over time. Furthermore, such interventions may have broader applications in neurological diseases characterized by barrier dysfunction. Thus, drug candidates that promote or restore blood-CNS barrier function are of high interest for the treatment of a range of prevalent retinal and neurological diseases.<sup>11</sup>

The major cellular components of the blood-CNS barriers are vascular ECs, which are supported by pericytes (PCs) and astrocytes. CNS ECs are characterized by efficient tight junctions, low rates of transcytosis, low rates of immune cell extravasation, and the expression of transporter proteins that provide specific transport mechanisms into and out of the CNS.<sup>12–14</sup> A central pathway for inducing and maintaining EC barrier functions is the beta-catenin-dependent (canonical) Wnt signaling pathway.<sup>15,16</sup> Among the 10 Wnt receptors of the Frizzled family, FZD4 is an important mediator of canonical signaling in the CNS vasculatures.<sup>17,18</sup> The best characterized ligands for FZDs in CNS ECs are Norrin – gene symbol

<sup>1</sup>Department of Ophthalmology and Visual Neurosciences, University of Minnesota, Minneapolis, MN, USA

<sup>2</sup>Graduate Program in Molecular, Cellular, Developmental Biology and Genetics, University of Minnesota, Minneapolis, MN, USA

<sup>3</sup>Department of Neuroscience, University of Minnesota, Minneapolis, MN, USA

<sup>4</sup>Department of Biochemistry, University of Toronto, Toronto, ON, Canada

<sup>5</sup>Terrence Donnelly Centre for Cellular and Biomolecular Research, Toronto, ON, Canada

<sup>6</sup>Leslie Dan Faculty of Pharmacy, University of Toronto, Toronto, ON, Canada

<sup>7</sup>Lead contact

\*Correspondence: zhangll@umn.edu (L.Z.), junge@umn.edu (H.J.J.)

<https://doi.org/10.1016/j.isci.2023.107415>



NDP<sup>19,20</sup> and WNT7A/B.<sup>16,21,22</sup> NDP is a non-Wnt protein released from multiple retinal and brain neural cell types, including horizontal cells, Müller cells, Bergman glia, and brain astrocytes.<sup>23–25</sup> It activates a receptor complex composed of FZD4, LRP5, and the tetraspanin-12 (TSPAN12) co-receptor<sup>26–28</sup> in ECs. WNT7A and WNT7B are released from neuroepithelium and mature neural cell types<sup>29</sup> and activate multiple FZD receptors, including FZD4. WNT7A/B signaling in ECs requires two additional membrane-associated proteins, GPR124 and RECK, for ligand-specific co-activation.<sup>30–39</sup> Gene ablation approaches in mice revealed the critical roles of NDP- and WNT7A/B-signaling systems in CNS angiogenesis and blood-CNS barrier function. Comparison of single and compound mutant mice affecting NDP or WNT7A/B signaling identified predominant roles of each signaling system in a CNS region-specific and developmental stage-specific manner (e.g., NDP-signaling in the developing and mature retina, WNT7A/B signaling in the developing medial ganglionic eminence) next to redundant roles (e.g., in the developing hindbrain and mature brain).<sup>40,41</sup>

Norrin and Wnt signaling in ECs has been studied for its roles in pathological retinal vasculature. For instance, transgenic Norrin overexpression reduced neovascularization (NV) in the oxygen-induced retinopathy (OIR) model<sup>42</sup> and FZD4-LRP5 agonists have a similar effect.<sup>43,44</sup> On the other hand, Chen et al. reported that expression of several Wnts is increased in the OIR model and that loss of Wnt signaling reduces NV in this model.<sup>45</sup> Together, these results highlight that context-dependent roles of Norrin and Wnt signaling, e.g., in developmental angiogenesis, quiescent vasculature, and pathological vasculatures, are very poorly understood and that developmental, protective, or pathological roles of the pathway need to be better defined.<sup>46</sup>

We recently reported the efficacy of a FZD4-LRP5 agonist, F4L5.13, in activating FZD4 signaling, promoting blood-CNS barrier function, and suppressing NV in the OIR model.<sup>43</sup> The agonist does not require the NDP co-receptor TSPAN12 for signaling initiation, which is exclusively required for NDP-induced FZD4 signaling.<sup>26,27,30,41</sup> F4L5.13 is a tetravalent engineered antibody modality<sup>47</sup> that binds FZD4 with sub-nanomolar affinity using two identical paratopes, and LRP5 with low nanomolar affinity using two distinct paratopes. F4L5.13 is selective for LRP5 over LRP6. F4L5.13 is a potent agonist for FZD4 in the presence of LRP5, presumably by mediating proximity of FZD4 and LRP5, leading to signal initiation.<sup>48</sup> Thus, it has properties of a canonical NDP mimetic. However, F4L5.13 is not expected to mimic potential functions of NDP that are FZD4-independent. F4L5.13 is expected to also mimic those WNT7A/B functions that are mediated by FZD4. Therefore, it is best described as a Frizzled-LRP agonist (FLAg) specific for FZD4. Before antibody-based agonists were available, beta-catenin gain-of-function approaches provided evidence for protective functions of canonical signaling in ECs in murine stroke models.<sup>34</sup> Recombinant NDP has been used to promote canonical signaling in ECs to antagonize VEGF-induced permeability.<sup>49</sup> Furthermore, viral gene delivery of engineered WNT7 variants was efficacious in normalizing barrier functions in mouse models of stroke and brain tumor models,<sup>50</sup> and a Frizzled4-selective Wnt surrogate improved outcomes in stroke models.<sup>51</sup> However, the biological basis of FZD4-LRP5 agonist activities in the CNS vasculature is not well understood. Furthermore, responsiveness of mature blood vessels is a critical prerequisite for therapeutic intervention, but if mature blood vessels are fully responsive to modulation by FZD4-LRP5 agonists is uncertain.<sup>43</sup>

Here, we find that F4L5.13 restores neural function in the *Tspan12* KO model of FEVR and that this effect correlates with restoration of developmental angiogenesis and alleviation of hypoxia. We define the developmental time window during which vascular and neural functions can be restored in *Tspan12* KO mice before the responsiveness of the maturing pathological vasculature decreases. Importantly, we find that mature blood vessels with barrier defects in a distinct disease model (late-induced *Tspan12* EC-specific KO mice) are fully responsive to F4L5.13. Single cell RNA-sequencing (scRNA-seq) reveals gene sets related to transport and BRB function that are dysregulated by loss of NDP/FZD4 signaling and restored by administration of agonist antibody. These gene sets provide detailed insights into the biological basis underlying the biological activity of a FZD4-LRP5 agonist and the role of beta-catenin-dependent FZD4 signaling in CNS ECs.

## RESULTS

### F4L5.13 restores developmental retinal angiogenesis

In the first week of murine postnatal life, the superficial vascular plexus extends radially from the optic nerve head toward the retinal rim. The formation of deep vascular networks (in the outer plexiform layer) and

intermediate capillary layers (in the inner plexiform layer) begins in the second week. In *Tspan12*<sup>-/-</sup> retinas, the deep vascular plexus never forms, and the intermediate and superficial vessels are malformed. In addition, the mutant mice display strong BRB defects.<sup>26,28</sup> We recently demonstrated that administration of F4L5.13 to postnatal *Tspan12*<sup>-/-</sup> mice restores developmental retinal angiogenesis and BRB formation but it appeared to have no effect on vascular density if administered to mature mice.<sup>43</sup> To better define the effects of F4L5.13 administration in restoring retinal angiogenesis, we administered the F4L5.13 in three distinct time windows (P6–P30, P15–P30, and P28–P42) to *Tspan12*<sup>-/-</sup> mice. While treatment from P6 to P30 is sufficient for full vascular restoration,<sup>43</sup> we continued treatment until P30 to conduct ERG and fluorescein angiography (FA) using mice with larger eyes. Optical sectioning of whole-mount retinas from *Tspan12* KO mice revealed that the development of intermediate and deep intraretinal capillary beds was virtually completely restored by F4L5.13 administration during the P6–P30 time window (Figure 1A). Quantification of the vascular area in the deep vascular layer revealed full restoration without excess vascularization (Figure 1B). Administration from P15 to P30 resulted in partial formation of deep layer capillaries (Figures 1C and 1D), and administration from P28 to P42 did not restore the deep layer vasculature (Figures 1E and 1F). Furthermore, administration of F4L5.13 from P24 to P40 in combination with an intravitreal injection of 1 µg of VEGF-164 at P27 was not sufficient to induce formation of the deep vascular plexus or resolve vascular malformations in the intermediate vascular plexus and at the vascular front (Figure S1A). To further investigate if F4L5.13 induces NV, we analyzed retinal sections. Misdirected angiogenesis or excess angiogenesis after prolonged F4L5.13 treatment was not observed and the results also corroborated the diminishing degree of vascular restoration in late treatment time windows (Figures S1B–S1D). Our findings extend earlier studies using inducible transgenic NDP overexpression and demonstrate that F4L5.13 administration is more effective in restoring retinal vascularization compared to transgenic overexpression of NDP from Müller glia.<sup>18</sup> The data define a developmental time window in which retinal angiogenesis can be stimulated by F4L5.13. Once this time window is closed, the F4L5.13 appears to be insufficient to induce angiogenesis, even in the presence of intravitreal VEGF-164. Our findings that F4L5.13 does not induce NV or restore angiogenesis in mature *Tspan12* KO mice is significant in the context of a potential use of Frizzled4 agonists as intervention in CNS vascular diseases, where the induction of NV would constitute an adverse effect.

### F4L5.13 restores retinal function in developing *Tspan12*<sup>-/-</sup> mice

Loss of NDP/FZD4 signaling causes a reduction of the ERG b-wave, which is generated by neural cells in the inner nuclear layer.<sup>52</sup> Conditional genetic disruption of NDP receptor complex components in ECs is sufficient to cause both vascular and ERG defects.<sup>17</sup> Scotopic ERGs revealed a strongly diminished ERG b-wave generated by *Tspan12*<sup>-/-</sup> retinas, while the a-wave was relatively normal (the trend toward a reduction of the a-wave was not significant). Administration of F4L5.13 from P6 to P30 fully restored the ERG b-wave (Figures 2A and 2B), indicating that retinal functional defects in *Tspan12*<sup>-/-</sup> mice are secondary to vascular defects, and that therapeutic approaches targeting EC-expressed receptors can result in profound improvements of neural functions.

To test if F4L5.13 treatment was effective in restoring the ERG of older *Tspan12*<sup>-/-</sup> mice, we administered the F4L5.13 from P15 to P30 and P28 to P42. We found that the ERG b-wave could still be largely restored during the P15–P30 time window (Figure 2C), however, administration from P28 to P42 was no longer effective (Figure 2D). These results are of interest in the context of therapeutic intervention in Norrie disease or FEVR, two related congenital diseases that are caused by mutations in genes mediating NDP/FZD4 signaling, including *TSPAN12*.<sup>53</sup>

To explore how retinal vascular defects cause secondary neural dysfunction, we injected mice with pimonidazole and probed retinal cross sections with hypoxyprobe mAb to detect the pimonidazole adducts formed in hypoxic tissue. Hypoxic areas in *Tspan12*<sup>-/-</sup> mice were detected in the inner nuclear layer, which is normally supplied by the flanking intraretinal deep and intermediate capillary beds (whereas the outer nuclear layer cells are predominantly supplied by choriocapillaris adjacent to the retinal pigment epithelium). Restoration of intraretinal capillaries by administration of F4L5.13 from P6 to P30 or P15 to P30 resulted in alleviation of hypoxia (Figures 3A and 3B), whereas administration from P28 to P42 did not restore intraretinal capillary formation or effectively alleviate hypoxia (Figure 3C). Furthermore, aberrant expression of the stress marker GFAP (glial fibrillary acidic protein) in Müller cells correlated with effective restoration of intraretinal capillaries (Figure S2). Thus, the developmental effects of the F4L5.13 on intraretinal capillary development and retinal function (ERG) are most likely linked by alleviation of hypoxia.

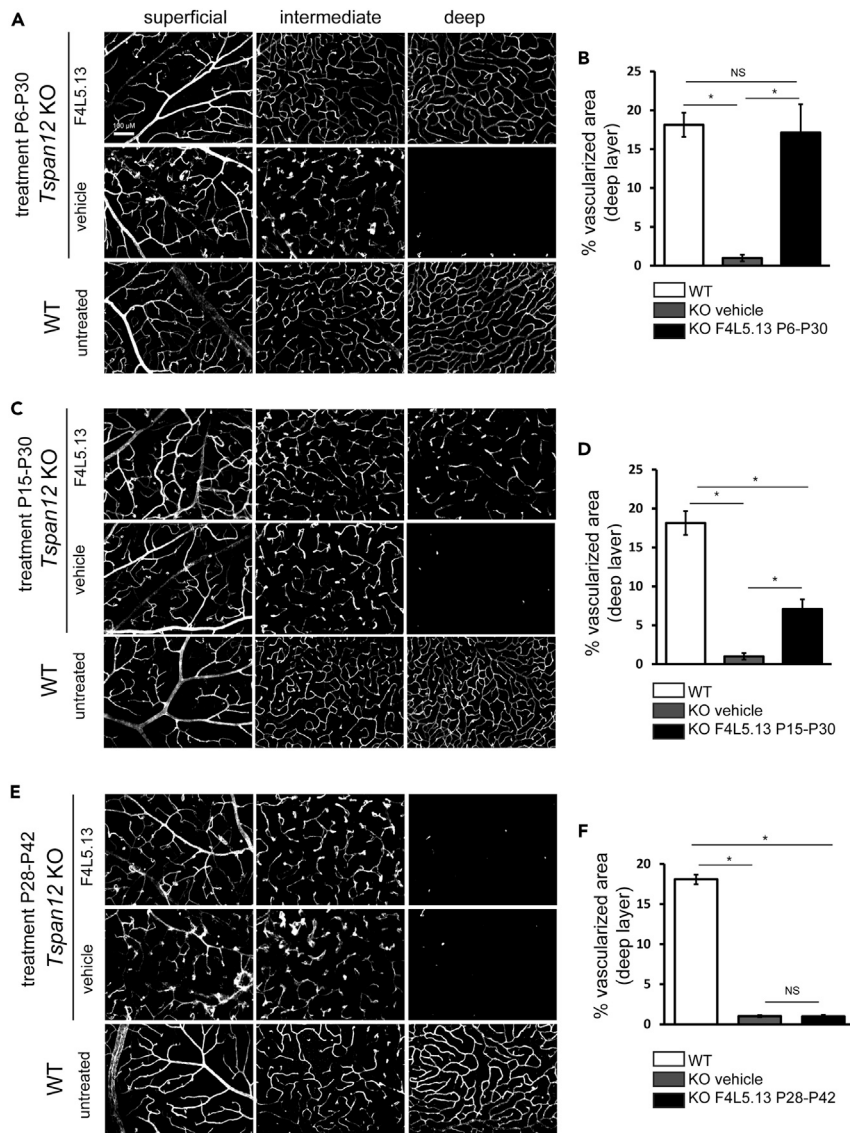


**Figure 1. F4L5.13 restores developmental angiogenesis in *Tspan12*<sup>-/-</sup> mice**

(A) Optical sectioning of vehicle treated *Tspan12* KO whole-mount retinas reveal a lack of deep layer capillaries in *Tspan12*<sup>-/-</sup> mice and that intermediate layer capillaries are malformed. F4L5.13 administration from P6 to P30 restores intraretinal capillary development to a degree comparable to wildtype controls. Scale bar: 100  $\mu$ m.

(B) Quantification of vascular area from  $n = 3-4$  mice. For each mouse, one retina was imaged, 5-6 images per retina were averaged. One-way ANOVA with Tukey post hoc, bars represent average  $\pm$  SD.

(C-F) The same analysis was performed for two different time windows of administration as indicated in the figure.

### F4L5.13 restores BRB function in developing and mature mice

Next, we determined if F4L5.13 can promote BRB functions of developing and mature blood vessels in the presence and absence of compounding pathologies. Interestingly, we found that the time window in which F4L5.13 can restore BRB function is distinct from the time window in which angiogenesis can be restored. FA revealed strong BRB defects in retinas of *Tspan12*<sup>-/-</sup> mice, which were fully restored by administration of the FLAg from P6 to P30 or P15 to P30. After administration from P28 to P42, a time window in which intraretinal angiogenesis and hypoxia can no longer be restored, BRB dysfunction was alleviated, and even administration from P60 to P75 resulted in attenuation of barrier dysfunction (Figure 4A). While both the P28-P42 and P60-P75-treated retinas are characterized by vascular malformations and hypoxia, the restorative effect of F4L5.13 in the P28-42 group was more pronounced than in the P60-P75 group.

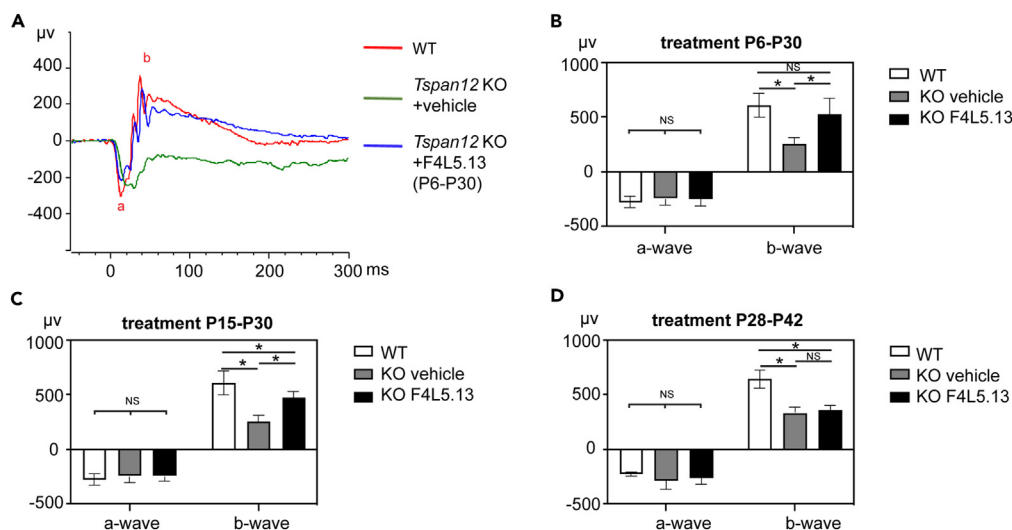


**Figure 2. F4L5.13 restores retinal function in developing *Tspan12*<sup>-/-</sup> mice**

(A) Example of scotopic electroretinograms recorded from the indicated groups at 1 cd\*s/m<sup>2</sup>. F4L5.13 administration was from P6-P30. Although treatment from P6-P20 is sufficient to restore the retinal vasculature in *Tspan12*<sup>-/-</sup> mice, the cohorts were treated until P30 when eyes were large enough to easily acquire ERGs.

(B) The b-wave is strongly reduced in ERGs obtained from P30 *Tspan12*<sup>-/-</sup> mice, administration of F4L5.13 from P6-P30 restores the ERG b-wave. N = 28 (control retinas), n = 12 (*Tspan12* KO retinas), n = 16 (F4L5.13-treated *Tspan12* KO retinas). One-way ANOVA with Tukey post hoc, bars represent average +/- SD.

(C) F4L5.13 administration from P15-P30 restores the b-wave in ERGs obtained from P30 *Tspan12*<sup>-/-</sup> mice. N = 28 (control), n = 12 (*Tspan12* KO), n = 10 (F4L5.13-treated *Tspan12* KO retinas). The same P30 WT and KO eyes were used in panel B and C. One-way ANOVA with Tukey post hoc, bars represent average +/- SD.

(D) F4L5.13 administration from P28-P42 does not substantially restore the b-wave in ERGs obtained from P42 *Tspan12*<sup>-/-</sup> mice. N = 4 (control retinas), n = 4 (*Tspan12* KO retinas), n = 7 (F4L5.13-treated *Tspan12* KO retinas). One-way ANOVA with Tukey post hoc, bars represent average +/- SD.

This finding suggests that the prolonged state of vascular dysfunction causes indirect pathological consequences that limit the full restoration of the BRB and/or that the drug-response of developing and mature blood vessels is not identical. Together, our observations indicate that (1) the time windows for restoring intraretinal capillary formation vs. promoting BRB function are not fully congruent, and (2) even in the presence of malformed blood vessels, hypoxia, and a prolonged state of vascular dysfunction, the BRB can be partially induced *de novo* by stimulating beta-catenin signaling.

To further investigate the BRB restoring effects of the F4L5.13 in mature blood vessels we turned to a model of *Tspan12* gene disruption without angiogenesis defects and the associated compounding pathologies. This model is generated by inducing the ablation of *Tspan12* in ECs at P28 (i.e., after vascular development is complete) using EC-specific and inducible Cdh5-CreERT2. Induction of recombination at P28 results in the maintenance of a virtually normal vascular architecture for at least 6 months after recombination in the presence of BRB defects.<sup>28</sup> The systemic *Tspan12* KO provides a model in which the BRB never forms in development. In contrast, the late-induced *Tspan12* EC-specific KO (iECKO) model is initially characterized by an intact barrier, which is however not fully maintained. By performing FA on systemic *Tspan12* KO mice and *Tspan12* iECKO mice (genotype: *Tspan12*<sup>f/f</sup>; Cdh5CreERT2<sup>+</sup>) we found that BRB defects in the iECKO mice are milder than in systemic *Tspan12* KO mice (Figure 5A). Furthermore, continuous monitoring of the same iECKO mice by FA revealed that the onset of barrier defects after tamoxifen-induced administration progressed over 2–3 months (Figure 5B). This finding indicates that a properly formed BRB in mature mice does not rapidly become dysfunctional upon reduction of NDP/FZD4 signaling. We found that Cdh5-CreERT2-induced recombination in adult retinal vascular ECs was efficient, yet it was not complete (Figure S3). To test if the remaining non-recombined ECs caused the milder BRB defects in *Tspan12* iECKO mice compared to systemic *Tspan12* KO mice, we performed additional experiments using *Tspan12*<sup>-/-</sup> mice restored with F4L5.13. After restoration of the retinal vasculature from P6 to P27, treatment with the F4L5.13 was discontinued, and the onset of BRB dysfunction was continuously monitored by FA. BRB

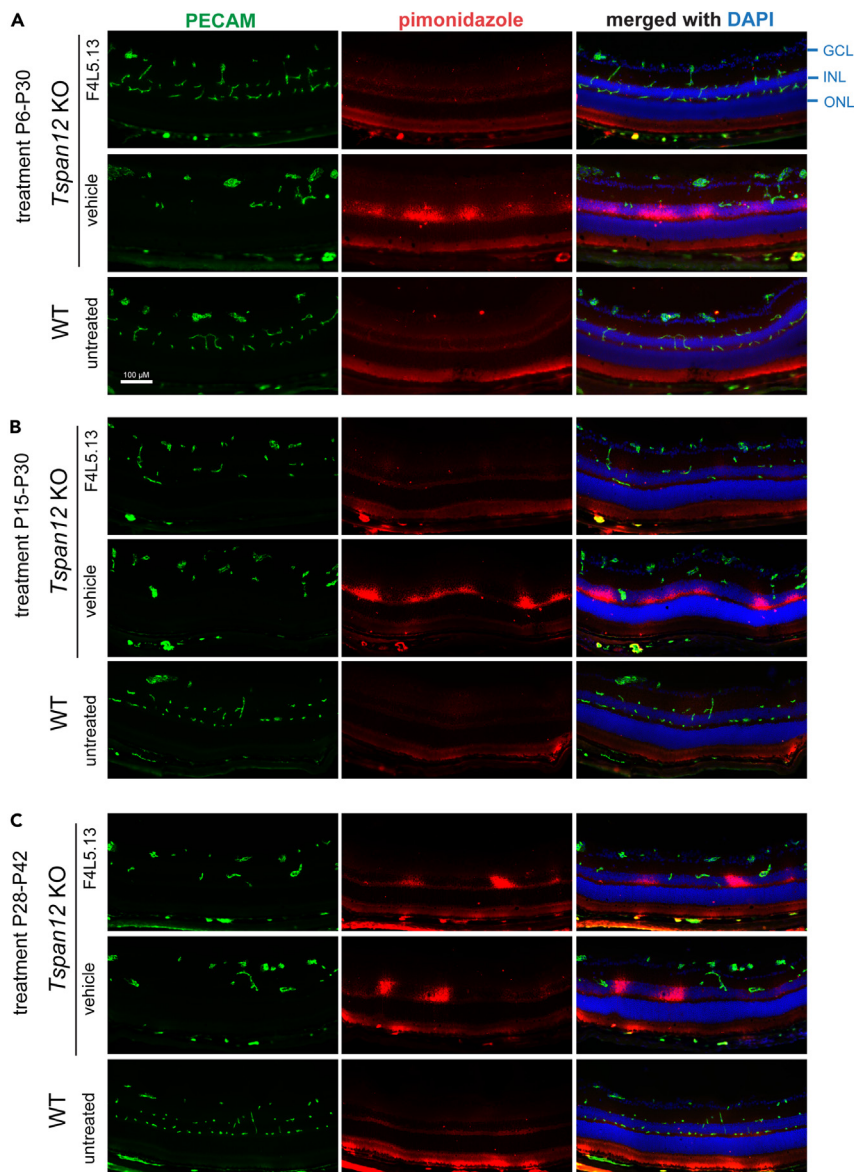


**Figure 3. F4L5.13 alleviates hypoxia in retinas of developing *Tspan12*<sup>-/-</sup> mice**

(A) Pimonidazole-adducts stained with Hypoxyprobe MAb reveal localized hypoxia in the inner nuclear layer of *Tspan12*<sup>-/-</sup> mice P30 retinas, especially in areas where intermediate layer capillaries do not compensate for the loss of deep layer capillaries. The outer nuclear layer is not hypoxic due to supply by the adjacent choriocapillaris. F4L5.13 administration from P6-P30 prevents the occurrence of hypoxia. GCL – ganglion cell layer, INL – inner nuclear layer, ONL – outer nuclear layer. Scale bar: 100 µm.

(B) Administration of F4L5.13 from P15-P30 alleviates hypoxia, the partially developed intraretinal capillary bed is largely sufficient to supply oxygen to the inner nuclear layer.

(C) Hypoxia remains after administration of F4L5.13 from P28-P42, albeit the extent appears reduced. Results in Figure 3 are representative of 3 independent experiments with similar results.

dysfunction manifested progressively as in *Tspan12* iECKO mice and did not nearly reach the same extent as observed in systemic *Tspan12*<sup>-/-</sup> mice (Figure 5C). Therefore, the strong BRB defects in *Tspan12*<sup>-/-</sup> mice may represent a compound phenotype, in which one component is directly related to loss of NDP/FZD4 signaling and target gene expression, and another component is associated with indirect pathological consequences of early angiogenesis defects. In addition, failure of BRB formation in development appears to cause more severe leakage than disturbed maintenance of the BRB.

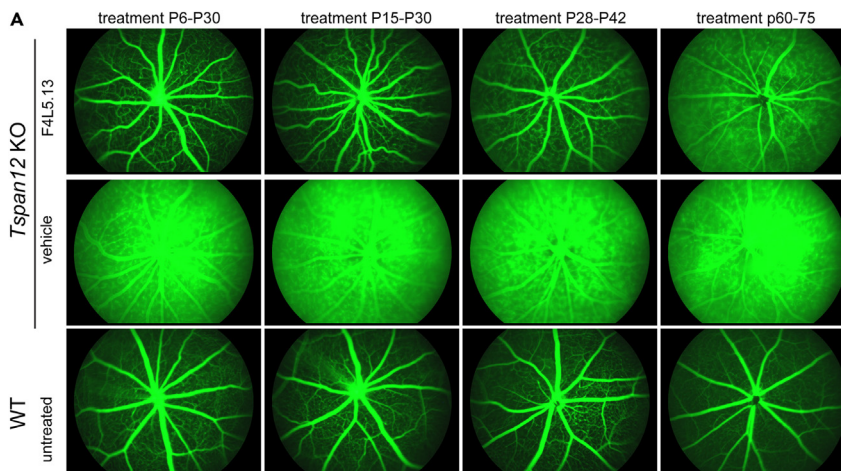


**Figure 4. F4L5.13 fully restores BRB function in developing *Tspan12*<sup>-/-</sup> mice and partially restores the BRB in mature mice**

(A) Fluorescein angiography images reveal strong BRB defects in *Tspan12*<sup>-/-</sup> mice. F4L5.13 administration from P6-P30 and P15-P30 restores BRB function virtually to the full extent, F4L5.13 administration from P28-P42 partially restores BRB function, and even in mature mice BRB function is enhanced by administration of F4L5.13. Results in Figure 4 are representative of 3–7 independent experiments with similar results.

In contrast to our results in systemic *Tspan12*<sup>-/-</sup> mice with compounding pathologies, administration of F4L5.13 to adult *Tspan12* iECKO mice (4 injections i.p., every two days) with properly formed blood vessels resulted in a striking degree of restoration of the BRB, suggesting that the role of FZD4 signaling in the mature BRB is profound (Figure 6A, see also Figure 4). In agreement with these data, we found that F4L5.13 more completely normalized PLVAP expression in mutant ECs of adult *Tspan12* iECKO mice, compared to mutant ECs of adult *Tspan12* systemic KO mice (Figure S4). Furthermore, we found that a single intravitreal dose of 2 μg F4L5.13 into the eyes of adult *Tspan12* iECKO mice rapidly (within 3 days) and profoundly restored BRB function (Figure 6B). The effect of the intravitreal injection diminished progressively; major BRB defects returned about 3–4 weeks after the single dose. These results are significant as they demonstrate that mature retinal blood vessels fully respond to F4L5.13 and that the intravitreal route of administration is effective, suggesting that local injection is an option to limit potential systemic effects of F4L5.13 administration. Given that BRB dysfunction is associated with macular edema, proliferative retinopathies and retinal occlusive diseases, these results highlight the potential of FZD4-LRP5 agonists to promote BRB function in ocular disease.

#### F4L5.13 decorates retinal vascular cells *in vivo*

We injected *Tspan12*<sup>-/-</sup> mice with a single dose of F4L5.13 (i.p.) and harvested the retinas 1 h later for immunostaining against the human Fc domain of F4L5.13. Retinal blood vessels (the images show retinal cross sections with blood vessels in the intermediate plexus) were decorated with F4L5.13 (Figure 7A), indicating that the F4L5.13 was bound to its EC-expressed receptors within 1 h of intraperitoneal injection. In the absence of F4L5.13 administration, no substantial immunoreactivity for F4L5.13 was observed (Figure 7B). These observations indicate that F4L5.13 binds to receptors on retinal ECs, consistent with its functional effects.

#### Biological basis of the activity of F4L5.13 in the retinal vasculature

To better understand the BRB and retinal functional phenotypes in *Tspan12*<sup>-/-</sup> retinas and the response to F4L5.13 treatment, we performed a scRNA-seq experiment using a droplet-based scRNA-seq platform. A total of 26,696 cells were sequenced from P26 WT, *Tspan12*<sup>-/-</sup> retinas and F4L5.13 treated *Tspan12*<sup>-/-</sup> retinas. The clusters on a t-distributed stochastic neighbor embedding (t-SNE) plot were matched to the major retinal cell populations based on known cell type markers (Figure 8A). ECs and PCs were not completely separated on t-SNE plots and therefore analyzed jointly as vascular cell population. When the individual retinal cells were color-coded by genotype/treatment group, a clear sub clustering within the Müller cell and bipolar cell populations became obvious, i.e., WT and treated cells overlapped, whereas the untreated

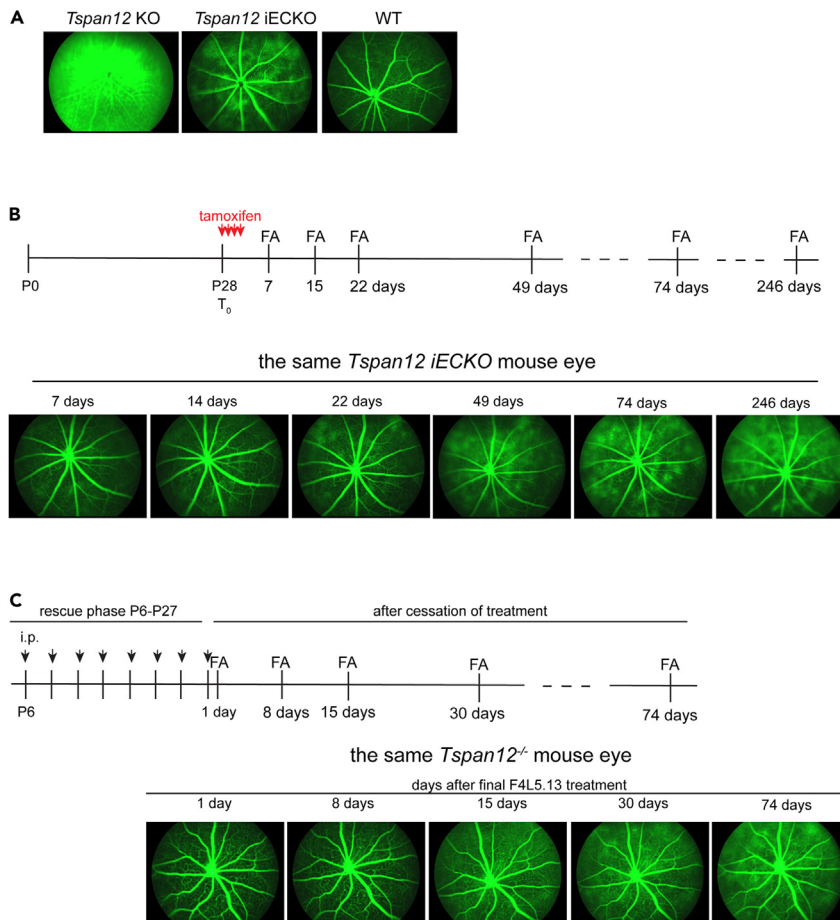


**Figure 5. Barrier defects caused by disruption of NDP/FZD4 signaling in developing vs. mature mice**

(A) Fluorescein angiography reveals quantitative differences between *Tspan12* KO mice and *Tspan12* iECKO mice. In *Tspan12* iECKO mice leakiness is milder than in *Tspan12* KO mice. *Tspan12* iECKO mice (*Cdh5creER*<sup>+</sup>; *Tspan12*<sup>f/f</sup>) are generated by inducing recombination at P28, i.e., after vascular development is complete, resulting in a model with barrier maintenance defects but otherwise intact vasculature.

(B) BRB dysfunction in the *Tspan12* iECKO model occurs in a slow and progressive manner after tamoxifen-induced recombination.

(C) A similar model of BRB defects is generated by a rescue/cessation of treatment approach in *Tspan12*<sup>-/-</sup> mice. Retinal vascular development is restored by F4L5.13 administration until P27. After cessation of treatment, progressive BRB dysfunction is monitored over time. The *Tspan12* gene is mutated in all endothelial cells in the rescue/cessation of treatment model, yet, the model has milder phenotypes than the systemic KO model, indicating that BRB defects are more severe in the presence of compounding vascular malformations. Results in Figure 5 are representative of at least 3 independent experiments with similar results.

*Tspan12*<sup>-/-</sup> cells were separated (Figure 8B). This separation indicates a substantial transcriptional dysregulation in *Tspan12*<sup>-/-</sup> retinas in inner nuclear layer cells and is consistent with the reduction of the ERG b-wave and localized hypoxia in the inner nuclear layer (Figure 3). FLAG-treated *Tspan12*<sup>-/-</sup> cells were largely overlapping with the corresponding wildtype cell populations, indicating a high degree of transcriptional normalization after F4L5.13 treatment.

We identified differentially expressed genes (DEGs) in Müller glia, bipolar cells, and vascular cells (WT vs. untreated KO) by performing ANOVA analysis and considered genes with p value <0.05 as differentially expressed. We highlight genes of interest (identified by gene set enrichment analysis or subjectively included) using heat maps. The DEGs in vascular cells (Figure 8C) were examined for established Wnt signaling response genes in retinal ECs (e.g., *Cldn5*, *Mfsd2a*, *Apcdd1*, *Lef1*, *Tnfrsf19*, *Tnfrsf21*, *Sox17*). These transcripts were reduced in *Tspan12*<sup>-/-</sup> vascular cells, whereas *Plvap* was increased, as expected. Among the

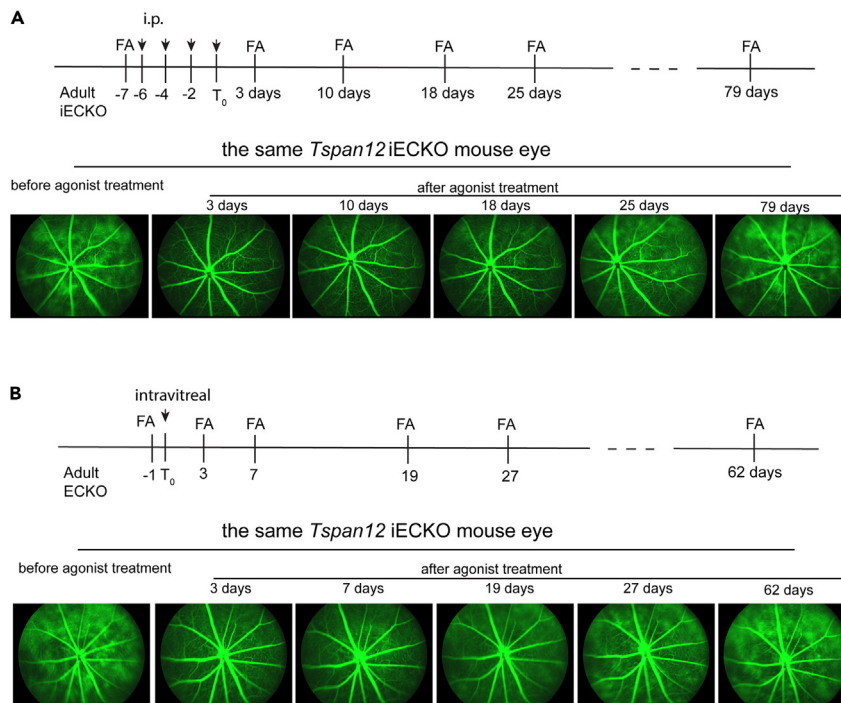


**Figure 6. A single intravitreal dose of F4L5.13 suppresses BRB dysfunction in *Tspan12* iECKO mice for several weeks**

(A) Four doses of F4L5.13 10 mg/kg i.p. fully restore BRB function in *Tspan12* iECKO mice. Continued monitoring reveals progressive return of BRB dysfunction starting about 3 weeks after cessation of treatment.  
(B) A single intravitreal dose of 2  $\mu$ g F4L5.13 suppresses BRB dysfunction in *Tspan12* iECKO mice for several weeks. Results in Figure 6 are representative of 3–6 independent experiments with similar results.

downregulated DEGs in mutant vascular cells were many mediators of transport and BRB function, i.e., gene products that limit unspecific extravasation (e.g., *Cldn5*, *Olc*, *Lsr/angulin-1*) or mediate specific transport (glucose, amino acids, lipids, vitamins, organic anions, and divalent cations). For example, the glucose transporter *Glut1/Slc2a1*, the amino acid transport mediators *Slc39a5* and *Slc7a1*, the lipid transporter *Mfsd2a*, the divalent cation transporter *Slc39a8/Zip8*, thiamine transporter *Slc19a3*, or the efflux pumps *Abcg2* and *Abcb1a/Pgp/Mdr* were reduced in *Tspan12*<sup>-/-</sup> vascular cells. Loss of NDP/FZD4 signaling is associated with reduced PC coverage of retinal blood vessels,<sup>17,28</sup> and PCs promote blood-CNS barrier function.<sup>54</sup> Wnt signaling in ECs was reported to induce a mediator of EC/PC interactions *Pdgfb*,<sup>34,55</sup> which we found downregulated in mutant vascular cells. *Vtn*, a matricellular protein expressed in PCs that regulates EC-mediated barrier functions,<sup>56</sup> was downregulated in *Tspan12*<sup>-/-</sup> vascular cells. Upstream of many of the DEGs may be transcription factors controlled by NDP/FZD4 signaling. Indeed, several transcription factors were found downregulated in *Tspan12*<sup>-/-</sup> vascular cells, including factors that are implicated in BBB maturation, e.g., *Irx3*, *Tbx1*, *Zic3*, and *Foxq1*.<sup>57,58</sup> Together, loss of *Tspan12* causes a very broad dysregulation of specific transport mechanisms and a simultaneous breakdown of mechanisms that limit unspecific extravasation, reflecting a fundamental and extreme dysfunction of the BRB.

Among the DEGs in Müller cells (Figure 8D) were several genes involved in glycolysis or the response to hypoxia, consistent with the hypoxia localized to the inner nuclear layer (Figure 3) and consistent with a previous scRNA-seq study on *Ndp*<sup>-/-</sup> mice.<sup>59</sup> Furthermore, multiple secreted modulators of the vasculature were upregulated, for example *Vegfa* and *Apln*. Several stress response genes and/or potential drivers of neural pathology were upregulated, including complement components *C3* and *C4b*, in support of our previous study on long-term pathological consequences of BRB defects.<sup>28</sup> Another population of inner nuclear layer cells, i.e., rod bipolar cells, also displayed dysregulation of hypoxia and glycolysis related genes (Figure 8E).

Consistent with the phenotypic restoration induced by F4L5.13, FLAg administration also resulted in widespread transcriptional normalization in ECs and Müller cells. For many genes, the normalization was partial

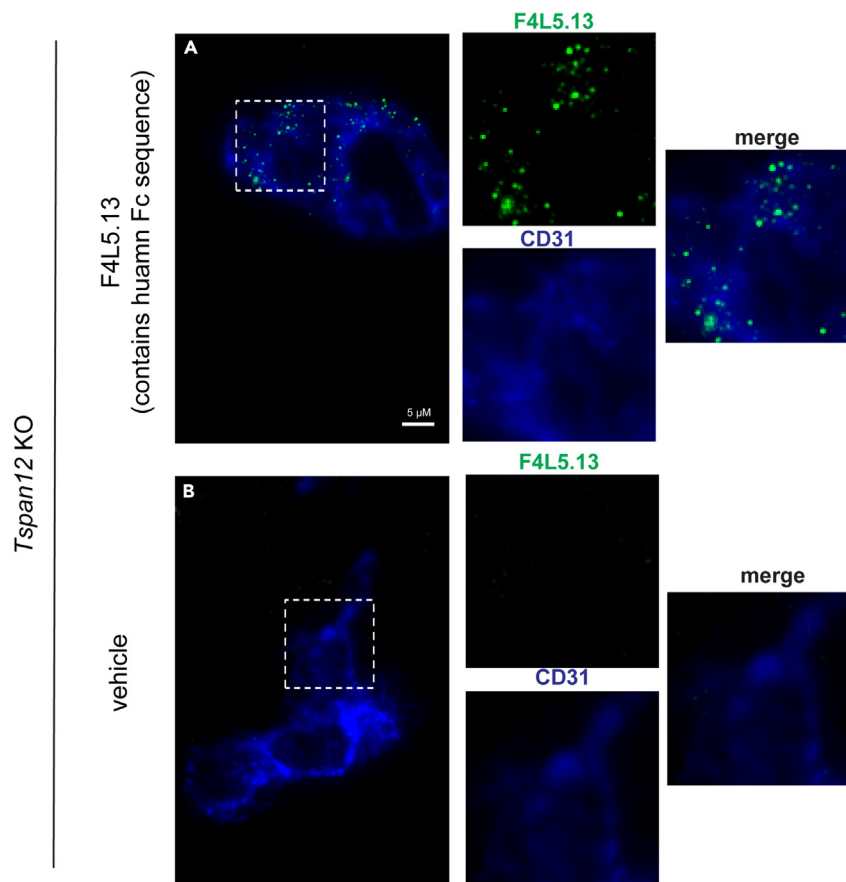


**Figure 7. F4L5.13 decorates retinal vascular cells after i.p. administration**

(A) One hour after i.p. injection, F4L5.13 tetrabody is detected with an anti-human Fc secondary. Images show retinal cross sections with blood vessels (imaged in the far-red channel, pseudo colored in blue) in the intermediate plexus. The punctate staining pattern occurs on retinal blood vessels.

(B) Anti-human Fc staining results in only faint fluorescence on specimens injected with vehicle.

to varying degrees, but only very few DEGs were not substantially restored by F4L5.13 (e.g., *Atp1a2*, *Fosl2*) whereas several genes were induced above the level of wild type control cells, among them transcription factors (*Foxq1*, *Irx3*, and *Tcf4*) as well as *Pdgfb*, *Tnfrsf19*, *Slc7a5*, and *Slc2a1*. The analysis of mutant vascular cells in conjunction with the restoration mediated by a FLaG is a powerful approach to identify genes expressed downstream of NDP/FZD4 signaling and to identify the biological basis of F4L5.13 activities.

## DISCUSSION

Agonists for the FZD4-LRP5/6 complex may provide a new approach to intervene in retinal and neurological diseases characterized by barrier breakdown or NV. F4L5.13 promotes BRB function and restores developmental retinal angiogenesis in *Tspan12*<sup>-/-</sup> mice but is not sufficient to activate angiogenesis of quiescent retinal vasculature in *Tspan12*<sup>-/-</sup> mice. Interestingly, FZD4 agonists also reduce pathological NV in the OIR model,<sup>43,44</sup> highlighting poorly understood context-dependent roles of canonical signaling in CNS ECs. Here, we defined the effects of F4L5.13 on the developing vs. mature retinal vasculature. F4L5.13 completely restores developmental angiogenesis in *Tspan12*<sup>-/-</sup> mice if it is administered from P6 onward. The time window for successful restoration of angiogenesis closes gradually between P15 and P28. F4L5.13 is not sufficient to promote angiogenesis in mature *Tspan12*<sup>-/-</sup> mice, although quiescent ECs clearly can respond to F4L5.13 by promoting barrier function. The restoration of developmental angiogenesis correlates with restoration of the ERG b-wave, most likely linked by the alleviation of hypoxia in the inner nuclear layer. Importantly, the experiments suggest that Norrin signaling is necessary for developmental angiogenesis but not sufficient to induce excess vascularization or normalize vascular density in mature hypo-vascular retinas.

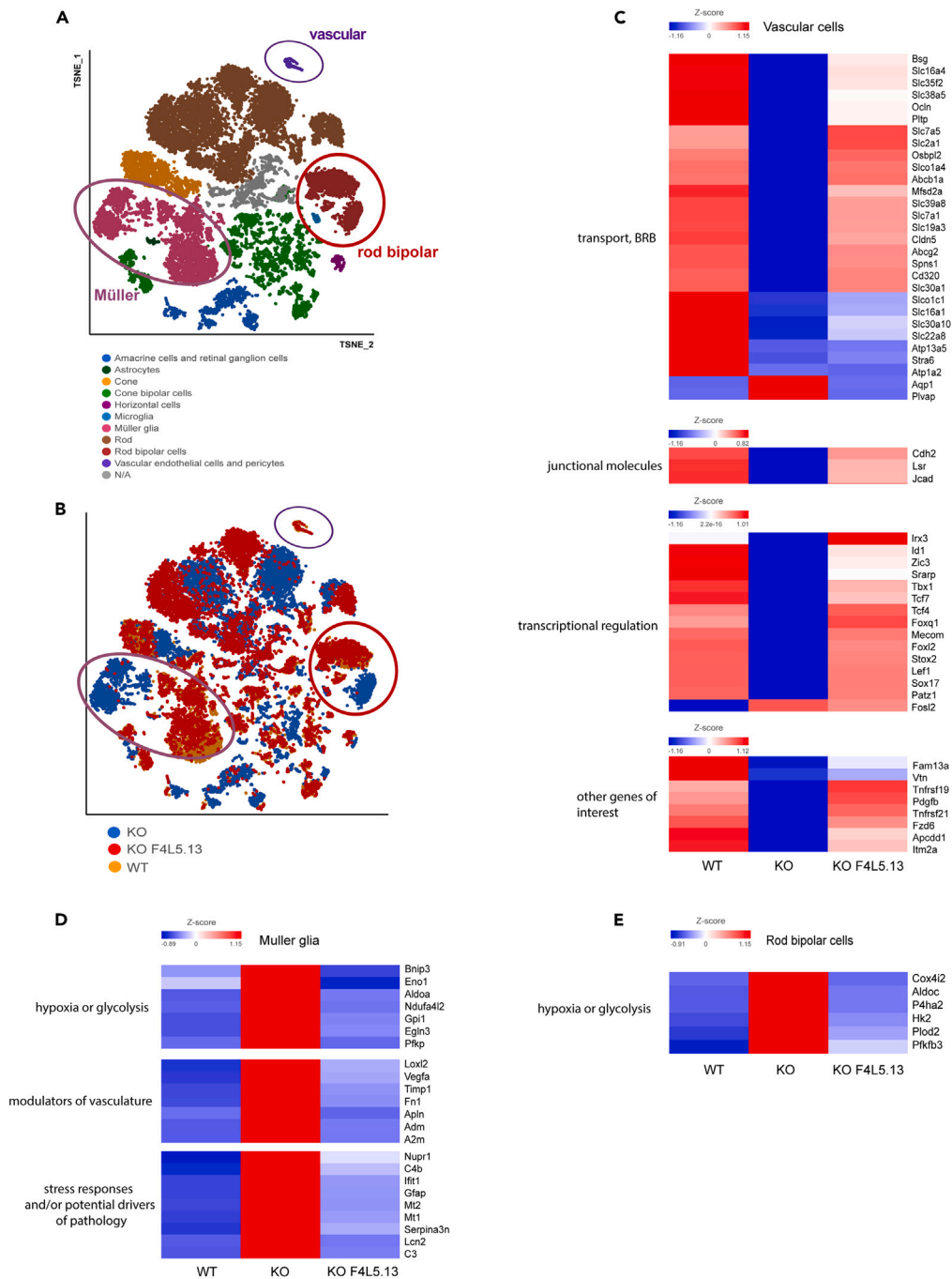


**Figure 8. ScRNA-seq analysis reveals the biological basis of F4L5.13 activity**

(A) t-SNE plot reveals clusters reflecting the major retinal cell populations.

(B) Color coding according to genotype and treatment reveals that Müller cells and rod bipolar cells (i.e., inner nuclear layer cells) are among the transcriptionally heavily dysregulated cell populations in *Tspan12*<sup>-/-</sup> retinas, whose expression is largely restored after F4L5.13 treatment.

(C) Genes of interest among vascular DEGs were highlighted by displaying them as heatmap. F4L5.13 treatment substantially normalizes gene expression of most vascular DEGs.

(D) Genes of interest among Müller glia DEGs. F4L5.13 treatment substantially normalizes gene expression of Müller glia DEGs.

(E) Genes of interest among rod bipolar cell DEGs.

Interestingly, the time window for restoring BRB function is distinct from the time window of restoring developmental angiogenesis. Between P28 and P42, i.e., in the presence of vascular malformations and hypoxia, the BRB remains substantially responsive to F4L5.13 administration, and even in mature animals the BRB can still be partially restored. Our study makes use of the finding that the BRB phenotypes can be separated from angiogenesis phenotypes by deleting *Tspan12* in ECs after vascular development is complete.<sup>28</sup> We found that the mature BRB of *Tspan12* iECKO mice, a model of impaired BRB maintenance without known compounding pathology, fully responds to F4L5.13. This finding suggests that secondary consequences of angiogenesis defects (e.g., hypoxia) limit the response to the FLAg in mature *Tspan12* KO mice and/or that disrupted barrier maintenance (in mature iECKO mice) is more easily corrected compared to secondarily inducing a barrier for the first time when initial barrier development did not occur (in mature systemic *Tspan12* KO mice). Analysis of *Tspan12* iECKO mice also reveals that BRB breakdown after tamoxifen-induced recombination is surprisingly slow and that it takes about 2–3 months before BRB defects develop to the full extent. A similar time course of BRB breakdown is observed in *Tspan12*<sup>-/-</sup> mice after cessation of F4L5.13 treatment. Importantly, a single intravitreal dose of F4L5.13 results in a rapid and profound restoration of BRB function for several weeks.

Our scRNA-seq data furthermore provide detailed insights into how NDP/FZD4 signaling promotes barrier function and how the FLAg restores it. Loss of NDP/FZD4 signaling causes an increase of unspecific extravasation due to impaired tight junctions (*Cldn5*, *Ocln*, and *Lsr*) and an increase of mediators of permeability (*Plvap* and *Aqp1*). Simultaneously, the expression of a broad array of specific transporters for required nutrients, vitamins, and ions is reduced. This massive breakdown of barrier functions is largely prevented if F4L5.13 is administered during retinal vascular development, and rapidly reversed in mature *Tspan12* iECKO mice after a single intravitreal injection of the agonist. These observations highlight the potential of Frizzled4 agonists for therapeutic intervention in retinopathies and neurological diseases characterized by barrier dysfunction, most prominently macular edema, and stroke. With respect to FEVR and Norrie disease, the potential use of FLAgs depends on several factors. Our studies in mice suggest that vascular density can only be restored in an early time window of development, thus diagnosis may come too late for an intervention that restores vascular density. However, FLAgs may alleviate BRB defects in FEVR patients and slow disease progression. In addition to the considerations of timing, the nature of the mutation in FEVR patients must also be considered. Frizzled4 agonists are expected to activate signaling when FEVR or Norrie disease is caused by mutations in *TSPAN12* or *NDP*, respectively. Mutated *FZD4* may also be activated, if one intact *FZD4* allele remains and is not indirectly affected by a dominant mutant allele, for example due to intracellular dimerization/trapping. In addition, those *FZD4* mutations that directly affect Norrin binding may remain capable to respond to a FLAg. Agonists for *FZD4* and *LRP6* may induce signaling in the presence of mutated *LRP5*, provided that sufficient levels of *LRP6* are expressed in the pathological retinal vasculature.

### Limitations of the study

In a hypothetical scenario where *FZD4* is expressed only on the basal surface of ECs, it needs to be considered how intraperitoneally administered F4L5.13 engages the receptor. Due to the severe BRB defects in our mouse models, F4L5.13 is expected to distribute to the vessel lumen as well as the basal extracellular space. With increasing restoration of the BRB, the distribution to the basal extracellular space may be increasingly limited. Whether *FZD4* has a polarized distribution in retinal ECs is not known and needs to be investigated in the future. Furthermore, technical improvements now allow for a better separation of ECs and PCs in scRNA-seq analyses so that transcriptional changes under control of *FZD4* can be determined in a cell-type specific manner in the future.

### STAR★METHODS

Detailed methods are provided in the online version of this paper and include the following:

- [KEY RESOURCES TABLE](#)
- [RESOURCE AVAILABILITY](#)
  - Lead contact
  - Materials availability
  - Data and code availability
- [EXPERIMENTAL MODEL AND STUDY PARTICIPANT DETAILS](#)
  - Animals
- [METHOD DETAILS](#)

- F4L5.13 antibody administration
- Electroretinography
- Immuno-staining and pimonidazole labeling of retinal tissue
- Fluorescein angiography
- Retinal cell dissociation for scRNAseq
- Single cell RNA-Seq library preparation for high-throughput sequencing
- Single-cell RNA-Seq data processing and analysis
- **QUANTIFICATION AND STATISTICAL ANALYSIS**
- Statistics

## SUPPLEMENTAL INFORMATION

Supplemental information can be found online at <https://doi.org/10.1016/j.isci.2023.107415>.

## ACKNOWLEDGMENTS

The authors would like to thank Heidi Röhrich for excellent histopathology support. This study was supported by the Regenerative Medicine Minnesota award (RMM 091620 DS 006 to HJJ), grants from the NIH (R01EY024261 and R01EY033316 to HJJ), and from the Canadian Institutes of Health Research (PJT-175160 to SA). HR was supported by P30EY011374, JL was supported by T32EY025187.

## AUTHOR CONTRIBUTIONS

H.J.J. and L.L.Z. designed experiments. L.L.Z., M.D.A., H.N.J., J.L., Q.C.D., Z.C., and H.J.J. conducted experiments and analyzed data. S.A. provided essential reagents. L.L.Z. and H.J.J. wrote the manuscript. All authors edited the manuscript.

## DECLARATION OF INTERESTS

S.A. is a shareholder of AntlerA Therapeutics and inventor on patent application 20210032352. H.J.J. is scientific advisor for AntlerA Therapeutics and received an honorarium.

## INCLUSION AND DIVERSITY

We worked to ensure sex balance in the selection of non-human subjects.

## DECLARATION OF GENERATIVE AI AND AI-ASSISTED TECHNOLOGIES IN THE WRITING PROCESS

None were used.

Received: February 11, 2023

Revised: May 22, 2023

Accepted: July 14, 2023

Published: July 18, 2023

## REFERENCES

1. Klaassen, I., Van Noorden, C.J.F., and Schlingemann, R.O. (2013). Molecular basis of the inner blood-retinal barrier and its breakdown in diabetic macular edema and other pathological conditions. *Prog. Retin. Eye Res.* 34, 19–48. <https://doi.org/10.1016/j.preteyeres.2013.02.001>.
2. Eshaq, R.S., Aldalati, A.M.Z., Alexander, J.S., and Harris, N.R. (2017). Diabetic retinopathy: Breaking the barrier. *Pathophysiology* 24, 229–241. <https://doi.org/10.1016/j.pathophys.2017.07.001>.
3. Díaz-Coránguez, M., Ramos, C., and Antonetti, D.A. (2017). The inner blood-retinal barrier: Cellular basis and development. *Vis. Res.* 139, 123–137. <https://doi.org/10.1016/j.visres.2017.05.009>.
4. Lendahl, U., Nilsson, P., and Betsholtz, C. (2019). Emerging links between cerebrovascular and neurodegenerative diseases—a special role for pericytes. *EMBO Rep.* 20, e48070. <https://doi.org/10.15252/embr.201948070>.
5. Sweeney, M.D., Sagare, A.P., and Zlokovic, B.V. (2018). Blood-brain barrier breakdown in Alzheimer disease and other neurodegenerative disorders. *Nat. Rev. Neurol.* 14, 133–150. <https://doi.org/10.1038/nrneuro.2017.188>.
6. Profaci, C.P., Munji, R.N., Pulido, R.S., and Daneman, R. (2020). The blood-brain barrier in health and disease: Important unanswered questions. *J. Exp. Med.* 217, e20190062. <https://doi.org/10.1084/jem.20190062>.
7. Zhao, Z., Nelson, A.R., Betsholtz, C., and Zlokovic, B.V. (2015). Establishment and Dysfunction of the Blood-Brain Barrier. *Cell* 163, 1064–1078. <https://doi.org/10.1016/j.cell.2015.10.067>.
8. Liebner, S., Dijkhuizen, R.M., Reiss, Y., Plate, K.H., Agalliu, D., and Constantin, G. (2018). Functional morphology of the blood-brain barrier in health and disease. *Acta*

- Neuropathol. 135, 311–336. <https://doi.org/10.1007/s00401-018-1815-1>.
9. Claesson-Welsh, L., Dejana, E., and McDonald, D.M. (2021). Permeability of the Endothelial Barrier: Identifying and Reconciling Controversies. *Trends Mol. Med.* 27, 314–331. <https://doi.org/10.1016/j.molmed.2020.11.006>.
  10. Apte, R.S., Chen, D.S., and Ferrara, N. (2019). VEGF in Signaling and Disease: Beyond Discovery and Development. *Cell* 176, 1248–1264. <https://doi.org/10.1016/j.cell.2019.01.021>.
  11. Yemanyi, F., Bora, K., Blomfield, A.K., Wang, Z., and Chen, J. (2021). Wnt Signaling in Inner Blood-Retinal Barrier Maintenance. *Int. J. Mol. Sci.* 22, 11877. <https://doi.org/10.3390/ijms222111877>.
  12. Obermeier, B., Daneman, R., and Ransohoff, R.M. (2013). Development, maintenance and disruption of the blood-brain barrier. *Nat. Med.* 19, 1584–1596. <https://doi.org/10.1038/nm.3407>.
  13. Langen, U.H., Ayloo, S., and Gu, C. (2019). Development and Cell Biology of the Blood-Brain Barrier. *Annu. Rev. Cell Dev. Biol.* 35, 591–613. <https://doi.org/10.1146/annurev-cellbio-100617-062608>.
  14. Ben-Zvi, A., and Liebner, S. (2022). Developmental regulation of barrier- and non-barrier blood vessels in the CNS. *J. Intern. Med.* 292, 31–46. <https://doi.org/10.1111/joim.13263>.
  15. Liebner, S., Corada, M., Bangsow, T., Babbage, J., Taddei, A., Czupalla, C.J., Reis, M., Felici, A., Wolburg, H., Fruttiger, M., et al. (2008). Wnt/beta-catenin signaling controls development of the blood-brain barrier. *J. Cell Biol.* 183, 409–417. <https://doi.org/10.1083/jcb.200806024>.
  16. Stenman, J.M., Rajagopal, J., Carroll, T.J., Ishibashi, M., McMahon, J., and McMahon, A.P. (2008). Canonical Wnt signaling regulates organ-specific assembly and differentiation of CNS vasculature. *Science* 322, 1247–1250. <https://doi.org/10.1126/science.1164594>.
  17. Ye, X., Wang, Y., Cahill, H., Yu, M., Badea, T.C., Smallwood, P.M., Peachey, N.S., and Nathans, J. (2009). Norrin, frizzled-4, and Lrp5 signaling in endothelial cells controls a genetic program for retinal vascularization. *Cell* 139, 285–298. <https://doi.org/10.1016/j.cell.2009.07.047>.
  18. Wang, Y., Rattner, A., Zhou, Y., Williams, J., Smallwood, P.M., and Nathans, J. (2012). Norrin/Frizzled4 signaling in retinal vascular development and blood brain barrier plasticity. *Cell* 151, 1332–1344. <https://doi.org/10.1016/j.cell.2012.10.042>.
  19. Xu, Q., Wang, Y., Dabdoub, A., Smallwood, P.M., Williams, J., Woods, C., Kelley, M.W., Jiang, L., Tasman, W., Zhang, K., and Nathans, J. (2004). Vascular development in the retina and inner ear: control by Norrin and Frizzled-4, a high-affinity ligand-receptor pair. *Cell* 116, 883–895.
  20. Ohlmann, A., and Tamm, E.R. (2012). Norrin: molecular and functional properties of an angiogenic and neuroprotective growth factor. *Prog. Retin. Eye Res.* 31, 243–257. <https://doi.org/10.1016/j.preteyeres.2012.02.002>.
  21. Noda, M., Vallon, M., and Kuo, C.J. (2016). The Wnt7's Tale: A story of an orphan who finds her tie to a famous family. *Cancer Sci.* 107, 576–582. <https://doi.org/10.1111/cas.12924>.
  22. Daneman, R., Agalliu, D., Zhou, L., Kuhnert, F., Kuo, C.J., and Barres, B.A. (2009). Wnt/beta-catenin signaling is required for CNS, but not non-CNS, angiogenesis. *Proc. Natl. Acad. Sci. USA* 106, 641–646. <https://doi.org/10.1073/pnas.0805165106>.
  23. Siegert, S., Cabuy, E., Scherf, B.G., Kohler, H., Panda, S., Le, Y.Z., Fehling, H.J., Gaidatzis, D., Stadler, M.B., and Roska, B. (2012). Transcriptional code and disease map for adult retinal cell types. *Nat. Neurosci.* 15, 487–495. <https://doi.org/10.1038/nn.3032>.
  24. Miller, S.J., Philips, T., Kim, N., Dastgheyb, R., Chen, Z., Hsieh, Y.C., Daigle, J.G., Datta, M., Chew, J., Vidensky, S., et al. (2019). Molecularly defined cortical astroglia subpopulation modulates neurons via secretion of Norrin. *Nat. Neurosci.* 22, 741–752. <https://doi.org/10.1038/s41593-019-0366-7>.
  25. Ye, X., Smallwood, P., and Nathans, J. (2011). Expression of the Norrie disease gene (*Ndp*) in developing and adult mouse eye, ear, and brain. *Gene Expr. Patterns* 11, 151–155. <https://doi.org/10.1016/j.gexp.2010.10.007>.
  26. Junge, H.J., Yang, S., Burton, J.B., Paes, K., Shu, X., French, D.M., Costa, M., Rice, D.S., and Ye, W. (2009). TSPAN12 regulates retinal vascular development by promoting Norrin-but not Wnt-induced FZD4/beta-catenin signaling. *Cell* 139, 299–311. <https://doi.org/10.1016/j.cell.2009.07.048>.
  27. Lai, M.B., Zhang, C., Shi, J., Johnson, V., Khandan, L., McVey, J., Klymkowsky, M.W., Chen, Z., and Junge, H.J. (2017). TSPAN12 Is a Norrin Co-receptor that Amplifies Frizzled4 Ligand Selectivity and Signaling. *Cell Rep.* 19, 2809–2822. <https://doi.org/10.1016/j.celrep.2017.06.004>.
  28. Zhang, C., Lai, M.B., Pedler, M.G., Johnson, V., Adams, R.H., Petrush, J.M., Chen, Z., and Junge, H.J. (2018). Endothelial Cell-Specific Inactivation of TSPAN12 (Tetraspanin 12) Reveals Pathological Consequences of Barrier Defects in an Otherwise Intact Vasculature. *Arterioscler. Thromb. Vasc. Biol.* 38, 2691–2705. <https://doi.org/10.1161/ATVBAHA.118.311689>.
  29. Biswas, S., Cottarelli, A., and Agalliu, D. (2020). Neuronal and Glial Regulation of CNS Angiogenesis and Barrierogenesis. *Development* 147. <https://doi.org/10.1242/dev.182279>.
  30. Zhou, Y., and Nathans, J. (2014). Gpr124 controls CNS angiogenesis and blood-brain barrier integrity by promoting ligand-specific canonical wnt signaling. *Dev. Cell* 31, 248–256. <https://doi.org/10.1016/j.devcel.2014.08.018>.
  31. Posokhova, E., Shukla, A., Seaman, S., Volate, S., Hilton, M.B., Wu, B., Morris, H., Swing, D.A., Zhou, M., Zudaire, E., et al. (2015). GPR124 Functions as a WNT7-Specific Coactivator of Canonical beta-Catenin Signaling. *Cell Rep.* 10, 123–130. <https://doi.org/10.1016/j.celrep.2014.12.020>.
  32. Eubelen, M., Bostaille, N., Cabochette, P., Gauquier, A., Tebabi, P., Dumitru, A.C., Koehler, M., Gut, P., Alsteens, D., Stainier, D.Y.R., et al. (2018). A molecular mechanism for Wnt ligand-specific signaling. *Science* 361, eaat1178. <https://doi.org/10.1126/science.aat1178>.
  33. Ulrich, F., Carretero-Ortega, J., Menéndez, J., Narvaez, C., Sun, B., Lancaster, E., Pershad, V., Trzaska, S., Véliz, E., Kamei, M., et al. (2016). RECK enables cerebrovascular development by promoting canonical Wnt signaling. *Development* 143, 147–159. <https://doi.org/10.1242/dev.123059>.
  34. Chang, J., Mancuso, M.R., Maier, C., Liang, X., Yuki, K., Yang, L., Kwong, J.W., Wang, J., Rao, V., Vallon, M., et al. (2017). Gpr124 is essential for blood-brain barrier integrity in central nervous system disease. *Nat. Med.* 23, 450–460. <https://doi.org/10.1038/nm.4309>.
  35. Vallon, M., Yuki, K., Nguyen, T.D., Chang, J., Yuan, J., Siepe, D., Miao, Y., Essler, M., Noda, M., Garcia, K.C., and Kuo, C.J. (2018). A RECK-WNT7 Receptor-Ligand Interaction Enables Isoform-Specific Regulation of Wnt Bioavailability. *Cell Rep.* 25, 339–349.e9. <https://doi.org/10.1016/j.celrep.2018.09.045>.
  36. Cho, C., Wang, Y., Smallwood, P.M., Williams, J., and Nathans, J. (2019). Molecular determinants in Frizzled, Reck, and Wnt7a for ligand-specific signaling in neurovascular development. *Elife* 8, e47300. <https://doi.org/10.7554/eLife.47300>.
  37. Vanhollebeke, B., Stone, O.A., Bostaille, N., Cho, C., Zhou, Y., Maquet, E., Gauquier, A., Cabochette, P., Fukuhara, S., Mochizuki, N., et al. (2015). Tip cell-specific requirement for an atypical Gpr124- and Reck-dependent Wnt/beta-catenin pathway during brain angiogenesis. *Elife* 4, e06489. <https://doi.org/10.7554/eLife.06489>.
  38. America, M., Bostaille, N., Eubelen, M., Martin, M., Stainier, D.Y.R., and Vanhollebeke, B. (2022). An integrated model for Gpr124 function in Wnt7a/b signaling among vertebrates. *Cell Rep.* 39, 110902. <https://doi.org/10.1016/j.celrep.2022.110902>.
  39. Junge, H.J. (2017). Ligand-Selective Wnt Receptor Complexes in CNS Blood Vessels: RECK and GPR124 Plugged In. *Neuron* 95, 983–985. <https://doi.org/10.1016/j.neuron.2017.08.026>.
  40. Zhou, Y., Wang, Y., Tischfield, M., Williams, J., Smallwood, P.M., Rattner, A., Taketo, M.M., and Nathans, J. (2014). Canonical WNT signaling components in vascular development and barrier formation. *J. Clin. Invest.* 124, 3825–3846. <https://doi.org/10.1172/JCI76431>.

41. Wang, Y., Cho, C., Williams, J., Smallwood, P.M., Zhang, C., Junge, H.J., and Nathans, J. (2018). Interplay of the Norrin and Wnt7a/Wnt7b signaling systems in blood-brain barrier and blood-retina barrier development and maintenance. *Proc. Natl. Acad. Sci. USA* 115, E11827–E11836. <https://doi.org/10.1073/pnas.1813217115>.
42. Ohlmann, A., Seitz, R., Braunger, B., Seitz, D., Bösl, M.R., and Tamm, E.R. (2010). Norrin promotes vascular regrowth after oxygen-induced retinal vessel loss and suppresses retinopathy in mice. *J. Neurosci.* 30, 183–193. <https://doi.org/10.1523/JNEUROSCI.3210-09.2010>.
43. Chidiac, R., Abedin, M., Macleod, G., Yang, A., Thibeault, P.E., Blazer, L.L., Adams, J.J., Zhang, L., Roehrich, H., Jo, H.N., et al. (2021). A Norrin/Wnt surrogate antibody stimulates endothelial cell barrier function and rescues retinopathy. *EMBO Mol. Med.* 13, e13977. <https://doi.org/10.15252/emmm.202113977>.
44. Nguyen, H., Chen, H., Vuppapalapaty, M., Whisler, E., Logas, K.R., Sampathkumar, P., Fletcher, R.B., Sura, A., Suen, N., Gupta, S., et al. (2022). SZN-413, a FZD4 Agonist, as a Potential Novel Therapeutic for the Treatment of Diabetic Retinopathy. *Transl. Vis. Sci. Technol.* 11, 19. <https://doi.org/10.1167/tvst.11.9.19>.
45. Chen, J., Stahl, A., Krah, N.M., Seaward, M.R., Joyal, J.S., Juan, A.M., Hatton, C.J., Aderman, C.M., Dennison, R.J., Willett, K.L., et al. (2012). Retinal expression of Wnt-pathway mediated genes in low-density lipoprotein receptor-related protein 5 (Lrp5) knockout mice. *PLoS One* 7, e30203. <https://doi.org/10.1371/journal.pone.0030203>.
46. Wang, Z., Liu, C.H., Huang, S., and Chen, J. (2019). Wnt Signaling in vascular eye diseases. *Prog. Retin. Eye Res.* 70, 110–133. <https://doi.org/10.1016/j.preteyeres.2018.11.008>.
47. Tao, Y., Mis, M., Blazer, L., Ustav, M., Jnr, Steinhart, Z., Chidiac, R., Kubarakos, E., O'Brien, S., Wang, X., Jarvik, N., et al. (2019). Tailored tetravalent antibodies potently and specifically activate Wnt/Frizzled pathways in cells, organoids and mice. *Elife* 8, e46134. <https://doi.org/10.7554/eLife.46134>.
48. Janda, C.Y., Dang, L.T., You, C., Chang, J., de Lau, W., Zhong, Z.A., Yan, K.S., Marecic, O., Siepe, D., Li, X., et al. (2017). Surrogate Wnt agonists that phenocopy canonical Wnt and beta-catenin signalling. *Nature* 545, 234–237. <https://doi.org/10.1038/nature22306>.
49. Díaz-Coránguez, M., Lin, C.M., Liebner, S., and Antonetti, D.A. (2020). Norrin restores blood-retinal barrier properties after vascular endothelial growth factor-induced permeability. *J. Biol. Chem.* 295, 4647–4660. <https://doi.org/10.1074/jbc.RA119.011273>.
50. Martin, M., Vermeiren, S., Bostaille, N., Eubelen, M., Spitzer, D., Vermeersch, M., Profaci, C.P., Pozuelo, E., Toussay, X., Raman-Nair, J., et al. (2022). Engineered Wnt ligands enable blood-brain barrier repair in neurological disorders. *Science* 375, eabm4459. <https://doi.org/10.1126/science.abm4459>.
51. Ding, J., Lee, S.J., Vlahos, L., Yuki, K., Rada, C.C., van Unen, V., Vuppapalapaty, M., Chen, H., Sura, A., McCormick, A.K., et al. (2023). Therapeutic blood-brain barrier modulation and stroke treatment by a bioengineered FZD(4)-selective WNT surrogate in mice. *Nat. Commun.* 14, 2947. <https://doi.org/10.1038/s41467-023-37689-1>.
52. Ruether, K., van de Pol, D., Jaissle, G., Berger, W., Tornow, R.P., and Zrenner, E. (1997). Retinoschisislike alterations in the mouse eye caused by gene targeting of the Norrie disease gene. *Invest. Ophthalmol. Vis. Sci.* 38, 710–718.
53. Gilmour, D.F. (2015). Familial exudative vitreoretinopathy and related retinopathies. *Eye (Lond)* 29, 1–14. <https://doi.org/10.1038/eye.2014.70>.
54. Armulik, A., Genové, G., Mäe, M., Nisanocioglu, M.H., Wallgard, E., Niaudet, C., He, L., Norlin, J., Lindblom, P., Strittmatter, K., et al. (2010). Pericytes regulate the blood-brain barrier. *Nature* 468, 557–561. <https://doi.org/10.1038/nature09522>.
55. Reis, M., Czupalla, C.J., Ziegler, N., Devraj, K., Zinke, J., Seidel, S., Heck, R., Thom, S., Macas, J., Bockamp, E., et al. (2012). Endothelial Wnt/beta-catenin signaling inhibits glioma angiogenesis and normalizes tumor blood vessels by inducing PDGF-B expression. *J. Exp. Med.* 209, 1611–1627. <https://doi.org/10.1084/jem.20111580>.
56. Ayloo, S., Lazo, C.G., Sun, S., Zhang, W., Cui, B., and Gu, C. (2022). Pericyte-to-endothelial cell signaling via vitronectin-integrin regulates blood-CNS barrier. *Neuron* 110, 1641–1655.e6. <https://doi.org/10.1016/j.neuron.2022.02.017>.
57. Sabbagh, M.F., Heng, J.S., Luo, C., Castanon, R.G., Nery, J.R., Rattner, A., Goff, L.A., Ecker, J.R., and Nathans, J. (2018). Transcriptional and epigenomic landscapes of CNS and non-CNS vascular endothelial cells. *Elife* 7, e36187. <https://doi.org/10.7554/eLife.36187>.
58. Hupe, M., Li, M.X., Kneitz, S., Davydova, D., Yokota, C., Kele, J., Hot, B., Stenman, J.M., and Gessler, M. (2017). Gene expression profiles of brain endothelial cells during embryonic development at bulk and single-cell levels. *Sci. Signal.* 10, eaag2476. <https://doi.org/10.1126/scisignal.aag2476>.
59. Heng, J.S., Rattner, A., Stein-O'Brien, G.L., Winer, B.L., Jones, B.W., Vernon, H.J., Goff, L.A., and Nathans, J. (2019). Hypoxia tolerance in the Norrin-deficient retina and the chronically hypoxic brain studied at single-cell resolution. *Proc. Natl. Acad. Sci. USA* 116, 9103–9114. <https://doi.org/10.1073/pnas.1821122116>.
60. Wang, Y., Nakayama, M., Pitulescu, M.E., Schmidt, T.S., Bochenek, M.L., Sakakibara, A., Adams, S., Davy, A., Deutsch, U., Lüthi, U., et al. (2010). Ephrin-B2 controls VEGF-induced angiogenesis and lymphangiogenesis. *Nature* 465, 483–486. <https://doi.org/10.1038/nature09002>.

## STAR★METHODS

### KEY RESOURCES TABLE

REAGENT or RESOURCE	SOURCE	IDENTIFIER
<b>Antibodies</b>		
Claudin 5-Alexa488	Invitrogen, Cat#352588	AB_2532189
PLVAP	BD Bioscience, Cat#550563	AB_393754
GFAP	Invitrogen, Cat#PA1-10019	AB_1074611
VE-Cadherin	BD Biosciences, Cat#555289	AB_395707
Pecam1	BD Biosciences, 550274	AB_393571
Human Fc	Jackson Immuno Research, Cat#109545008	AB_2337833
CD73	Biolegend, Cat#127202	AB_1089066
<b>Chemicals, peptides, and recombinant proteins</b>		
F4L5.13	AntlerA Therapeutics, under MTA	N/A
Rat VEGF-164 Protein	R&D Systems, Cat#564-RV	N/A
<b>Experimental models: Organisms/strains</b>		
Mouse: Tspan12 <sup>f</sup> :B6-Tspan12 <sup>tm1.1Hjug</sup>	<a href="https://doi.org/10.1161/ATVB.AHA.118.311689">https://doi.org/10.1161/ATVB.AHA.118.311689</a>	MMRRC_046319-UNC
Mouse: Tspan12 <sup>f</sup> :B6-Tspan12 <sup>tm1.2Hjug</sup>	<a href="https://doi.org/10.1161/ATVB.AHA.118.311689">https://doi.org/10.1161/ATVB.AHA.118.311689</a>	N/A
Mouse: Cdh5creER <sup>+</sup> :Tg(Cdh5-cre/ERT2)1Rha	<a href="https://doi.org/10.1038/nature09002">https://doi.org/10.1038/nature09002</a>	N/A
<b>Software and algorithms</b>		
Partek Flow	Partek Incorporated, Version 9.0	N/A
<b>Deposited data</b>		
Single-cell RNA-Seq data	NCBI, GEO	GSE213887
<b>Other</b>		
Chromium Single Cell 3' library & Gel Bead kit v3	10x Genomics, Cat#1000075	N/A
Pierce Protein A/G Magnetic Beads	Thermo Scientific, Cat#88802	N/A
Papain	Worthington Biochemical Corporation, Cat#LK003176	N/A
DNase I	Worthington Biochemical Corporation, Cat#LK003170	N/A
Collagenase type 4	Worthington Biochemical Corporation, Cat#LS004186	N/A
Ovomucoid	Worthington Biochemical Corporation, Cat#LK003182	N/A
Ames' medium	Sigma, Cat#A1420	N/A
AK-Fluor fluorescein	Akorn, Cat#17478-253-10	N/A
Pimonidazole	Hypoxypore Inc., Cat#HP7 100 kit	N/A
Hamilton syringe	Hamilton, Cat#7653-01	N/A
Hamilton needle	Hamilton, Cat#7803-05	N/A
1% tropicamide	Sandoz, NDC 61314-355-02	N/A
2.5% phenylephrine	Akorn, NDC 17478-201-15	N/A
Erythromycin ophthalmic ointment 0.5%	Bausch & Lomb, NDC 24208-910-55	N/A
Griffonia simplicifolia Isolectin B4-Alexa 647	Invitrogen, Cat# 132450	SCR_014365
Annexin V	Biolegend, Cat#640904	N/A
Protein A	Cytiva, Cat#17127903	N/A

### RESOURCE AVAILABILITY

#### Lead contact

Further information and requests for resources and reagents should be directed to and will be fulfilled by the lead contact Harald Junge ([junge@umn.edu](mailto:junge@umn.edu)).

### Materials availability

This study did not generate new unique reagents.

### Data and code availability

- scRNA-seq data have been deposited at NCBI GEO under accession number GSE213887, which is publicly available.
- This study does not report original code.
- Any additional information required to reanalyze the data reported in this paper is available from the [lead contact](#) upon request.

## EXPERIMENTAL MODEL AND STUDY PARTICIPANT DETAILS

### Animals

*Tspan12* floxed (*Tspan12*<sup>tm1.1Hj<sup>ug</sup></sup>) and null (*Tspan12*<sup>tm1.2Hj<sup>ug</sup></sup>) alleles were reported previously and maintained on a C57BL/6J background.<sup>28</sup> Rosa mT/mG reporter mice were obtained from Jackson Laboratories. Recombination of *Tspan12*<sup>fl/+</sup>; Cre<sup>+</sup> mice was induced at P28 with four intraperitoneal injections of 100  $\mu$ L tamoxifen in cornoil (20 mg/ml) every 2 days. Tg(*Cdh5-cre*/ERT2)1Rha<sup>50</sup> was used as Cre driver. Animals of both sexes were used for all studies. Mice from P6 to nine month old were used, ages of mice are detailed in each figure. Mice were housed in a specific pathogen-free animal facility. All animal protocols were approved by the Animal Care and Use Committee of the University of Minnesota, Twin Cities.

## METHOD DETAILS

### F4L5.13 antibody administration

F4L5.13 was produced as previously described.<sup>43</sup> In brief, two plasmids encoding F4L5.13 polypeptide chains were expressed in Expi293F suspension cells and purified via ProteinA. The polypeptide chains dimerize via the Fc/Fc knobs-in-whole interface as well as the V<sub>H</sub>/V<sub>L</sub> interface to form the tetravalent antibody modality. F4L5.13 or vehicle were administered either intraperitoneally (10 mg/kg at P6, P9, P12, thereafter 4 mg/kg every three days for developing mice; 4 doses of 10 mg/kg for mature mice) or intravitreally (2  $\mu$ g in a volume of 1  $\mu$ l). For intravitreal delivery, mice were anesthetized using an isoflurane gas delivery system, pupils were dilated with a 1:1 mix of 1% tropicamide and 2.5% phenylephrine. A 33-gauge needle (Hamilton, 7803-05) with micro syringe (Hamilton, 7653-01) was used to penetrate the sclera approximately 1 mm behind the limbus, and 1  $\mu$ l of F4L5.13 (2  $\mu$ g/ $\mu$ l) or vehicle was injected slowly into the vitreous cavity. To reduce reflux, the needle was retrieved slowly 30 seconds after injection, then erythromycin ophthalmic ointment 0.5% (Bausch & Lomb) was applied to the injection area of the eye. For intravitreal injection of VEGF-164, 1  $\mu$ l of rat VEGF-164 (R+D Systems, 564-RV) at a concentration of 1  $\mu$ g/ $\mu$ l was injected.

### Electroretinography

Mice were dark-adapted overnight and electroretinograms were acquired under red light. Mice were anesthetized using isoflurane gas. Pupils were dilated with a 1:1 mix of 1% tropicamide and 2.5% phenylephrine immediately after anesthesia was induced. After the pupils were fully dilated, hypromellose lubricant eye gel (Systane gel) was applied to keep both corneas moistened. ERGs were acquired on the heated platform of a Celeris Diagnosys ERG system. Impedance was 5-15 K $\Omega$ . Eyes were stimulated at 1 cd s/m<sup>2</sup>.

### Immuno-staining and pimonidazole labeling of retinal tissue

Mice were anesthetized using an isoflurane drop jar and then euthanized by cervical dislocation. Eyes were dissected and immediately frozen (unfixed) in optimal cutting temperature compound (OCT; Tissue-Tek), using a cryomold placed into a container filled with 2-methylbutane, which was placed into liquid nitrogen. 12  $\mu$ m sections were cut and placed onto microscope slides, which were immersed in 4% PFA for 10 min at RT, or ice-cold methanol for 10 min at -20°C, for fixation. Sections were blocked for 30 min with 5% goat serum in PBS with 0.1% Triton X-100, and incubated with antibodies in blocking buffer for 1 hour at RT. The primary antibodies used in this study were: anti-Claudin 5-Alexa488 (1:100, Invitrogen, 352588), anti-PLVAP (1:100, BD Bioscience, 550563), anti-GFAP (1:200, Invitrogen, PA1-10019), anti-VE-Cadherin (1:200, BD, 555289) and Griffonia Simplicifolia Isolectin B4-Alexa 647 (1:100, Invitrogen, 132450), anti-Pecam1 (1:50, BD Biosciences, 550274). 60 mg/kg pimonidazole (Hypoxyprobe Inc., HP7-100 kit) was

intraperitoneally injected into mice 3 hours before sacrificing the mice. Anti-pimonidazole (1:200, Hypoxyprobe Inc., HP7-100 kit) was used to stain the pimonidazole adducts. For retinal wholemounts, PFA fixed retinas were blocked for 1 hour at RT (5% goat serum in PBS with 0.5% Triton X-100) and stained with primary antibody overnight at 4°C and with secondary antibody for 2 hours at RT, with at least 5 10-min-long washes in PBS 0.5% TritonX-100. For quantification of the vascular area in the outer plexiform layer, 3D image stacks were acquired using a Keyence BZX800 microscope. Multiple optical sections—which collectively contained the deep layer capillaries—were combined into a maximum intensity projection, which was subjected to thresholding. The vascularized area (IB4 signal above the threshold) was determined using ImageJ software. For immunostaining of F4L5.13, 10 mg/kg F4L5.13 was injected i.p. into adult *Tspan12<sup>-/-</sup>* mice and eyes were harvested 1 hour later. 12 μm unfixed sections were obtained as described above and fixed for 10 min in ice cold methanol, washed in PBS, and blocked and stained as described above, using anti human Fc (Jackson Immuno Research, 109545008). Images were obtained using a Keyence BZ-X810 digital microscope.

### Fluorescein angiography

Mice were anesthetized using an isoflurane gas delivery system. Pupils were dilated with a 1:1 mix of 1% tropicamide and 2.5% phenylephrine immediately after anesthesia was induced. After dilation, SYSTANE ULTRA lubricant eye drops were applied to keep the cornea moistened. 10 μl/g bodyweight of 0.25% fluorescein (diluted in sterile saline 0.9% from 10% Fluorescein-sodium, Akorn) was administered subcutaneously. Images were acquired 5 minutes after the fluorescein administration using a Micron III rodent fundus imaging system (Phoenix). Post-FA, mice were placed on a heating pad for recovery.

### Retinal cell dissociation for scRNAseq

Immediately after euthanization, eyeballs were dissected and placed into ice-cold Ames' solution (Sigma, A1420). Retinas were dissected and then digested in papain solution (20 units/ml papain, Worthington Biochemical Corporation, LK003176), 0.005% DNase I (Worthington Biochemical Corporation, LK003170), and 200 units/ml Collagenase type 4 (Worthington Biochemical Corporation, LS004186) in Ames' solution) at 37°C for 15 min with constant agitation. After digestion, the tissue was triturated with a p1000 pipet tip 10-20 strokes to break up larger tissue fragments. Cells were pelleted at 300 g for 5 min at 4°C, the supernatant discarded, and the cell pellet immediately resuspended in 1 ml upper gradient solution (1 mg/ml albumin, 1 mg/ml ovomucoid inhibitor, LK003182, 0.005% DNase I, in Ames' solution, equilibrated with 95% O<sub>2</sub>, 5% CO<sub>2</sub> gas). The cell suspension was passed through a 50 μm cell strainer. To remove debris, the 1 ml cell suspension was carefully placed over 5 ml of lower gradient solution (i.e., 10 mg/ml albumin, 10 mg/ml ovomucoid inhibitor in Ames' solution) and centrifuged at 100 g for 6 minutes at 4°C (whole cells were pelleted, while membrane fragments remained at the interface). The supernatant was discarded, and the pelleted cells were resuspended in 1 ml upper gradient solution. To remove photoreceptors and dead cells, the cell suspension was incubated with magnetic beads coupled with anti-CD73 (Biolegend, 127202) and Annexin V (Biolegend 640904) at 4°C for 20 min with end-to-end mixing. After removing the magnetic beads with a magnetic stand, the supernatant was pelleted at 300 g for 5 min at 4°C. The pelleted cells were resuspended in upper gradient solution and counted using a LOGOS cell counter. Cell preparations with 60-80% viability were used for further library construction and sequencing.

### Single cell RNA-Seq library preparation for high-throughput sequencing

Single-cell suspensions were adjusted to a final concentration of 50,000 cells in 50 μl and filtered using pluuriStrainer mini (50 μm, pluuriSelect, Germany). Single cell reverse transcription and cDNA synthesis was performed using a Chromium platform (10x Genomics) and Chromium Single Cell 3' library & Gel Bead kit v3 (10x Genomics, 1000075) following the manufacturer's instructions. Samples were indexed using Single Index Kit T Set A (10x Genomics). An appropriate sequencing library size range and the cDNA concentration were determined using an Agilent 2100 Bioanalyzer. The libraries were sequenced at Novogene using Illumina HiSeq system, with 150 bp paired end read length at a 50,000 reads/cell sequencing depth.

### Single-cell RNA-Seq data processing and analysis

Single-cell RNA-Seq data analysis was performed using Partek Flow software (Version 9.0, Partek Incorporated). After filtering out nucleotide barcodes that correspond to empty droplets, aligned reads were quantified to generate a single cell count matrix. 24071 genes and 26696 single cells (6092 cells in WT

group, 10769 cells in *Tspan12* KO group, and 9835 cells in F4L5.13-treated *Tspan12* KO group) were included in the analysis. Unsupervised Graph-based clustering was used, and results were visualized in t-SNE plots. Retinal cell populations were defined based on known marker genes. Genes with p-value < 0.05 were identified as DEGs.

## QUANTIFICATION AND STATISTICAL ANALYSIS

### Statistics

ERG data were normally distributed. Multiple group comparisons were performed using one-way analysis of variance with Tukey posthoc,  $p < 0.05$  was considered significant. Statistical details can be found in the figure legends. Statistical calculations were performed using the Statistics Kingdom web app.